

A Versatile Synthetic Route to Phosphonate-Functional Monomers, Oligomers, Silanes, and Hybrid Nanoparticles

Martin Schmider,^{*,†} Ekkehard Müh,[†] Joachim E. Klee,[‡] and Rolf Mülhaupt[†]

Institut für Makromolekulare Chemie und Freiburger Materialforschungszentrum der Albert-Ludwigs-Universität, Stefan-Meier-Strasse 31, D-79104 Freiburg im Breisgau, Germany, and Dentsply DeTrey GmbH, De-Trey-Strasse 1, D-78467 Konstanz, Germany

Received December 1, 2004; Revised Manuscript Received August 20, 2005

ABSTRACT: The highly selective single Michael addition of diethyl vinylphosphonate to alkylamines represents a very versatile synthetic route affording a large variety of novel multifunctional phosphonates including aminoalkylphosphonates, phosphonate functional silanes, and phosphonate-functionalized acrylic monomers. The hydrolysis of the phosphonate group results in a phosphonic acid functional monomer which can be used as component of dental composites exhibiting improved filler–matrix interaction. The sol–gel reaction of the phosphonate-functional silanes produced novel phosphonate-functional organic/inorganic hybrid nanoparticles with particle sizes ranging from 30 to 100 nm.

Introduction

Dimethacrylates are widely used for matrixes of dental materials in conjunction with photoinitiators, silane interfacial coupling agents, and functionalized silica fillers.^{1–4} The properties of such composite materials are greatly influenced by both the filler dispersion and the interfacial adhesion of the dispersed inorganic filler. Dispersion problems are frequently encountered when using nanometer-scaled filler particles due to their very strong interparticle interactions. An important objective in dental chemistry is to combine properties of polymers and ceramics by preparing organic/inorganic hybrid systems via sol/gel chemistry. Sol/gel chemistry is the key to preparing inorganic particles with variable surface functionality including core/shell-type particles.⁵ In preferred compositions, micro- and nanometer-scaled particles are attached to the acrylic organic matrix via covalent or ionic bond formation, respectively.⁶ The covalent interfacial coupling is achieved when acrylic silanes are copolymerized. New families of acrylic nanocomposites with improved matrix/filler adhesion were prepared from sol/gel reactions of bismethacrylate silanes.^{7–10} As displayed in Scheme 1, the bismethacrylate silanes are obtained when ethylene glycol acrylate methacrylate (EGAMA) is reacted with aminoalkylsilanes. Below room temperature, the acrylate group reacts selectively with the primary amines. Exclusive 2-fold Michael addition accounts for the formation of bismethacrylate silanes. In this molecular tool box approach, the structures of the amines can be varied over a very wide range. Although covalent interfacial coupling is very effective, the ionomer coupling also offers attractive potential. According to a recent study, the incorporation of phosphonic acids into the acrylic monomer promotes both biocompatibility and adhesion of the dental materials to the teeth because calcium phosphonates and phosphonate complexes are formed.^{11,12} However, most of the state-of-the-art acrylic phosphonates require tedious multistep syntheses.^{13–15} Here we report an expanded molecular tool box approach toward

phosphonate-functional acrylics, silanes, and organic/inorganic hybrid nanoparticles. This expanded molecular tool box is based upon the Michael addition of diethyl vinylphosphonate to various amines including aminoalkylsilanes. Special emphasis is being placed upon the syntheses and characterization of novel phosphonate intermediates in one-pot reactions. Moreover, the multifunctional phosphonate silanes were used in dual cure reactions, combining sol/gel condensation with free radical polymerization, to prepare nanocomposites. Both phosphonate-functional intermediates and phosphonate-functional nanoparticles were examined as new interfacial coupling agents in dental composites.

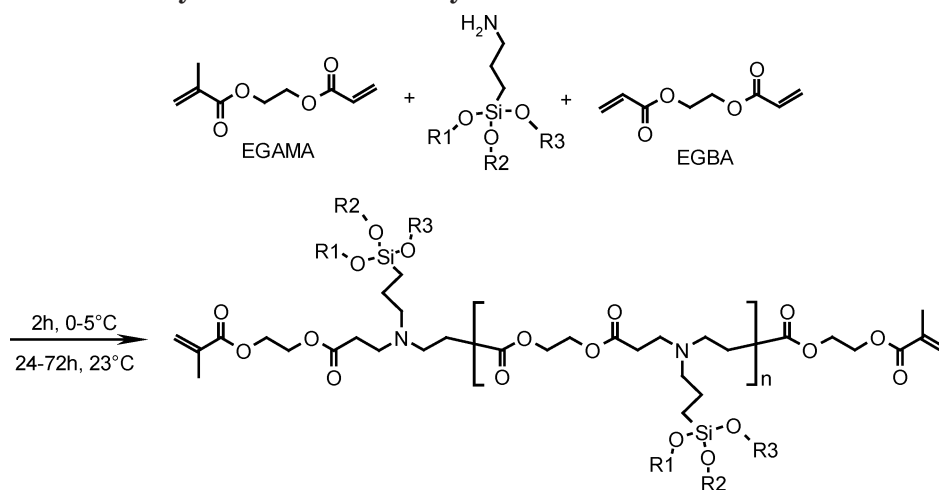
Results and Discussion

A. Monomers. A novel class of phosphonate-functional acrylic monomers were prepared according to the general synthetic route shown in Scheme 2. Key feature of the synthesis of phosphonate monomers (**1a–c**) was the Michael addition of a variety of primary amines to the vinyl group of diethyl vinylphosphonate. For all monomers, the conversion of the vinyl group in the course of the Michael addition was monitored by ¹H and ¹³C NMR spectroscopy. The addition reaction was commonly complete after 24 h at 70 °C, as evidenced by the disappearance of the ¹H NMR signals of the vinyl group at 6.19, 6.04, and 5.97 ppm as well as the ¹³C NMR signals at 135.3 and 126.1 ppm. At the same time characteristic signals appeared at 1.94 and 2.85 ppm in the ¹H NMR spectra and at 27.0 and 42.1 ppm in the ¹³C NMR spectra, respectively, which can be assigned to the new aliphatic bond. In ¹³C NMR, the characteristic doublet shifts from 126.1 to 27.0 ppm due to the hetero-coupling between the C-nucleus and the P-nucleus. NMR spectroscopy provides evidence that in the case of the addition product **1b** the alkoxy silane groups were not affected during Michael addition. In contrast to the 2-fold Michael addition of acrylate groups, exclusive monoaddition was observed for the vinylphosphonate addition to the amines displayed in Table 1. The GC–MS spectra of addition products **1a** and **1b** typically show the expected molecular ions [MH⁺] at *m/z* 272 (**1a**) and 386 (**1b**), in accord with the formation of monoaddition product. Besides GC–MS,

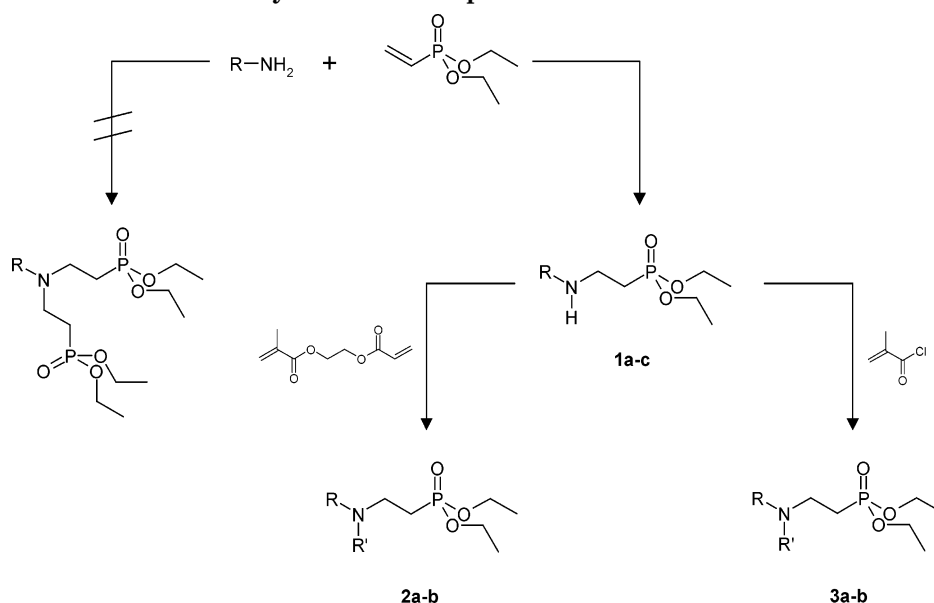
[†] Institut für Makromolekulare Chemie und Freiburger Materialforschungszentrum der Albert-Ludwigs-Universität.

[‡] Dentsply DeTrey GmbH.

Scheme 1. Synthesis of Bismethacrylatesilanes via 2-Fold Michael Addition



Scheme 2. Synthesis of Phosphonate-Functional Monomers



also MALDI-TOF measurements confirmed the exclusive formation of monoaddition product by reaction of bis(aminopropyl)-terminated oligo(propylene oxide) (Jeffamine) with diethyl vinylphosphonate (Figure 1). The maxima of the signals in the MALDI-TOF spectrum of **1c** were shifted to higher m/z compared to the maxima of the signals in the spectrum of Jeffamine (Figure 2). The difference corresponds exactly to the 2-fold molecular weight of diethyl vinylphosphonate, i.e., monoaddition of every amine group of the oligomer with diethyl vinylphosphonate has occurred.

The monomers **2a,b** were prepared by selective Michael addition of **1a** respectively **1b** to the acrylate functionalities of 2-(acryloyloxy)ethyl methacrylate. 2-(acryloyloxy)ethyl methacrylate was prepared according to a procedure published by Moszner et al.¹⁶ The rate of the reaction was monitored by ¹H NMR spectroscopy. During the Michael addition, the signals of the acrylate group at 6.5, 6.1, and 5.8 ppm decreased. Typical new signals occurred at 2.6 and 2.2 ppm, which are due to the new aliphatic bond. The same phenomenon was observed by ¹³C NMR spectroscopy. During the Michael addition, the signals of the acrylate group at 131 and 128 ppm shifted to 50 and 32 ppm in the spectra. Besides ¹H NMR, ¹³C NMR and FAB-MS

measurements confirmed the formation of the expected monomers **2a,b**. The FAB-MS spectra show molecular ions [MH⁺] at m/z 456 (**2a**) and 570 (**2b**), confirming the formation of addition products with EGAMA. This is shown in Figure 3 by the FAB-MS spectrum of the monomer **2b**.

The novel α,β -unsaturated amides **3a,b** were prepared according to a procedure published by Rodriguez

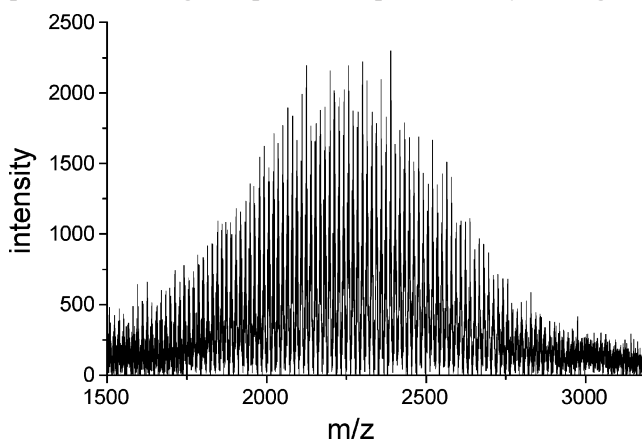
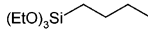
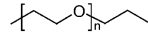
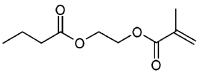
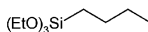
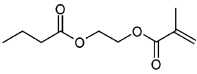
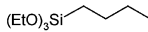
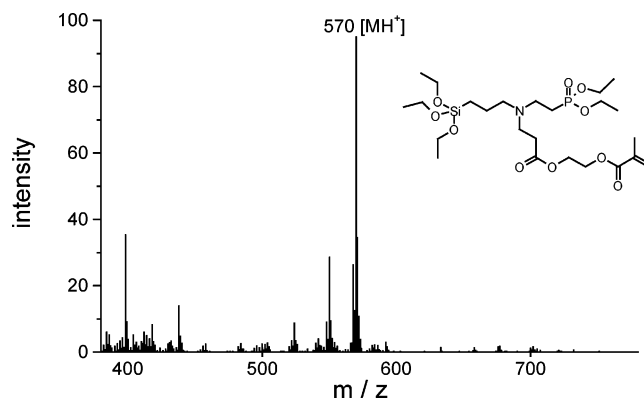


Figure 1. MALDI-TOF spectrum of **1c**.

Table 1. Monomers **1a–c**, **2a–b**, and **3a–b** Prepared via Michael Addition and Amidation

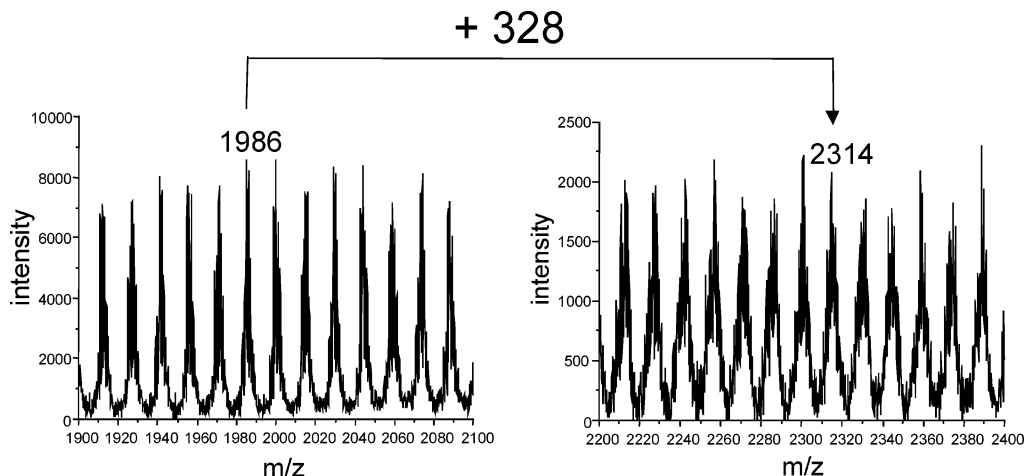
Monomer	R	R'
1a		H
1b		H
1c		H
2a		
2b		
3a		
3b		

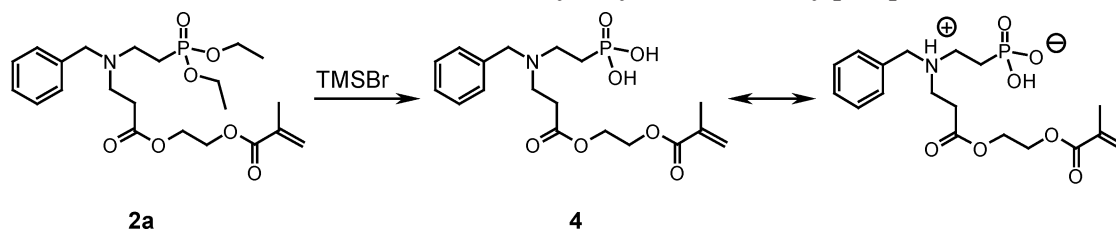
et al.¹⁷ and characterized by NMR spectroscopy. In ¹H NMR, typical new signals corresponding to the methyl groups next to the N-nucleus, previously observed at 2.52 and 2.81 ppm, were afterward shifted to 3.28 and 3.53 ppm (**3a**). The same phenomenon was observed for monomer **3b**. The signals were shifted from 2.81 and 3.68 ppm to 3.59 and 4.72 ppm. This is due to the improved shielding of the nuclei after amidation. Furthermore, the ethoxy-substituted alkoxy silane groups of **3b** remained uncondensed as evidenced by the existence of the ¹H NMR signals at 1.3 and 3.8 ppm as well as the ¹³C NMR signals at 18.3 and 58.5 ppm. The reaction of bromotrimethylsilane with the dialkylphosphonate **2a** and the hydrolysis of the resultant silyl phosphonate were carried out to prepare the Zwitterionic aminoalkylphosphonic acid **4** under very mild conditions (Scheme 3). The spectral properties of **4** strongly supported the hydrolysis of the dialkylphosphonate **2a**. In particular the ³¹P NMR was most informative, since the resonance due to the phosphonate

**Figure 3.** FAB-MS spectrum of monomer **2b**.

2a was observed at $\delta = 31.1$ ppm whereas in the phosphonic acid **4** the resonance was found at $\delta = 19.2$ ppm.

B. Nanoparticles. The new phosphonate-functionalized acrylic silanes can be condensed to form silicate nanoparticles with reactive acrylate and phosphonate surfaces. First the sol-gel condensation of phosphonate-functionalized acrylic silane **2b** was carried in the presence of 3 wt % aqueous HF solution and ethyl acetate as solvent. After stirring for 2 days at room temperature, volatile components such as ethyl acetate and water were removed under vacuum. Condensation product of **2b** (**CP_{2b}**) was mixed with Bis-GMA/TGDMA and then polymerized by free radical polymerization in order to covalently attach the particles to the matrix. After the resulting composite was milled, the obtained nanocomposite powder was characterized by solid state ²⁹Si cross-polarization magic angle spinning (CP MAS) NMR spectroscopy. Figure 4 shows the spectrum of **CP_{2b}**. Formation of the silica network was evidenced by the dominant NMR signal at -67.1 ppm, corresponding to the Si bonded through O atoms to three other Si (T^3). Signals in the range of -58 , -50 , and -42 ppm corresponding to Si bonded to two (T^2), only one (T^1) or even no further Si (T^0) were not detected, confirming the cross-linked structure. Furthermore, the condensation product **CP_{2b}** was characterized by transmission electron microscopy (TEM). Figure 5 shows the TEM image of condensation product of **2b** (**CP_{2b}**). According to the analysis of numerous TEM images, the particles formed have diameters in the range of 30 to 100 nm.

**Figure 2.** Zoom of MALDI-TOF spectra of unmodified Jeffamine (left) and **1c** (right).

Scheme 3. Reaction Scheme of the Hydrolysis of the Dialkylphosphonate **2a**

In a second approach silicate nanoparticles were formed by co-condensation of silane **2b** with tetraethyl orthosilicate (TEOS) in different ratios as shown in Table 2. The condensation reactions were carried out again in the presence of 3 wt % aqueous HF solution

and ethyl acetate as solvent. The morphology of the samples was detected by means of TEM. Figure 5 shows the TEM image of condensation product of **2b** with TEOS in ethyl acetate (**CP_{2b}-TEOS-3**) containing hybriide nanoparticles with diameters ranging from 30 to 60 nm.

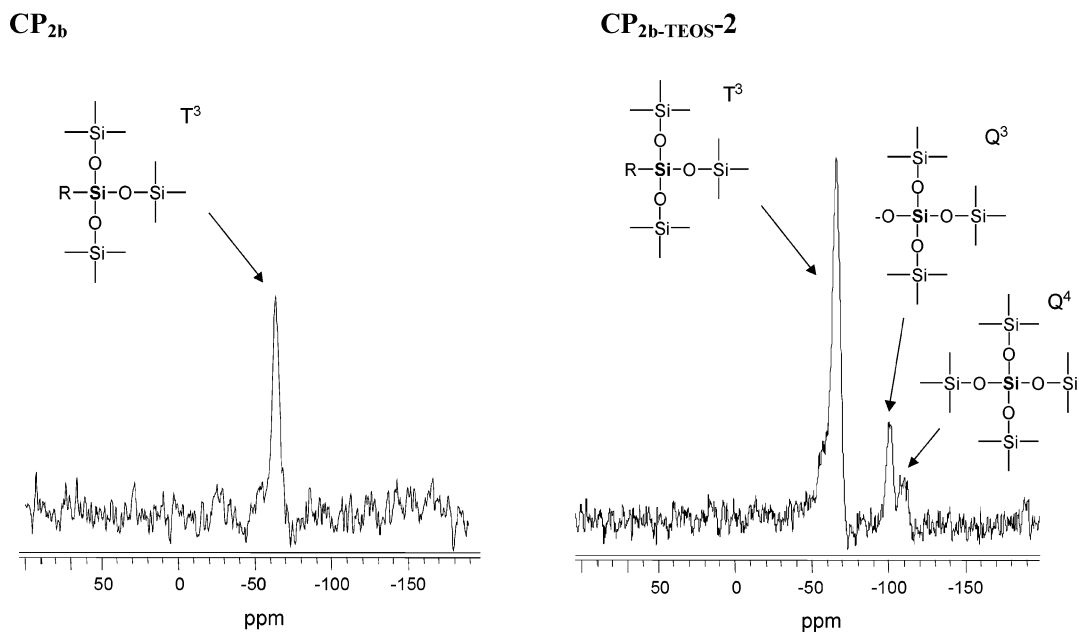


Figure 4. ²⁹Si (CP MAS) NMR spectra of condensation products **2b** (**CP_{2b}**) and (**CP_{2b}-TEOS-2**).

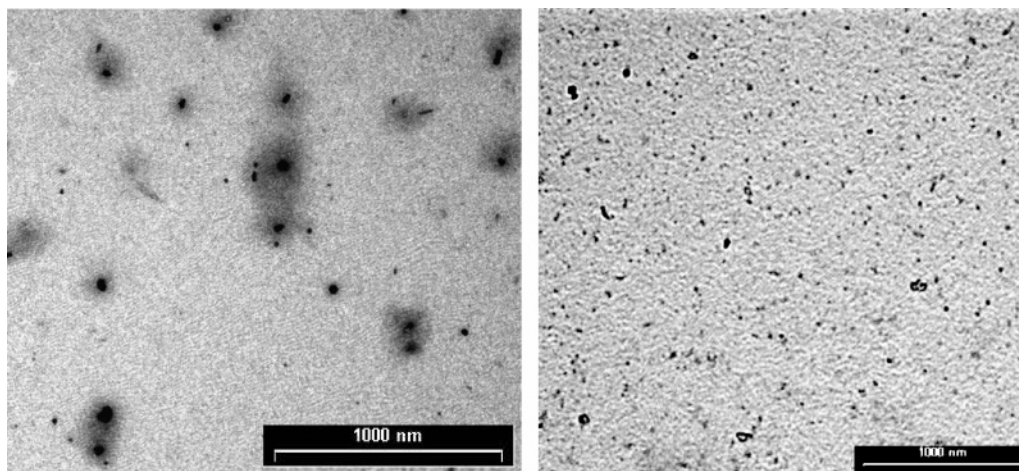


Figure 5. TEM images of the nanoparticle dispersions **CP_{2b}** and **CP_{2b}-TEOS-3**.

Table 2. Mechanical Properties of Condensation Products **CP_{2b}-TEOS-x** and Bis-GMA/TGDMA

condensation product	2b /TEOS [mol/mol]	SiOR/H ₂ O [mol/mol]	SiOR/H ⁺ [mol/mol]	compressive strength [MPa]	flexural strength [MPa]
Bis-GMA/TGDMA (70/30 w/w)				235 ± 12	60 ± 4
CP_{2b}-TEOS-1	4.0	1.0	1.0	110 ± 18	6 ± 2
CP_{2b}-TEOS-2	1.8	1.0	1.0	140 ± 20	7 ± 3
CP_{2b}-TEOS-3	1.1	1.0	1.0	140 ± 21	9 ± 5
CP_{2b}-TEOS-4	0.7	1.0	1.0	160 ± 26	12 ± 3

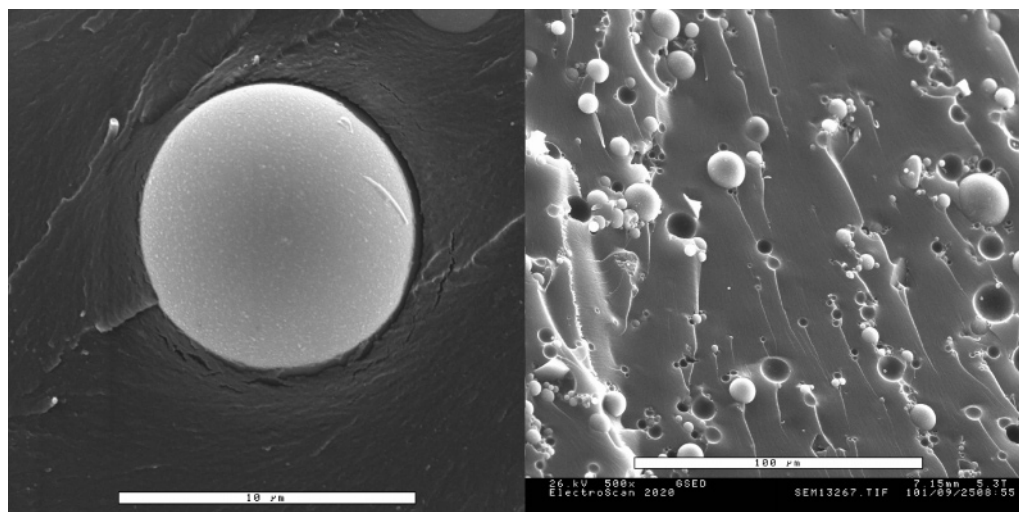


Figure 6. Fracture surface of the composite **FC-MS-0**.

Table 3. Mechanical Properties of Composites without Monomer 4 (**FC-MS-0**) and with Monomer 4 (**FC-MS-1** and **FC-MS-5**)

	composite			
	Bis-GMA/TGDMA (70/30)	FC-MS-0	FC-MS-1	FC-MS-5
monomer 4 [wt %]	0	0	1	5
Bis-GMA/TGDMA (70/30) [wt %]	100	80	79	75
filler content [wt %]	0	20	20	20
viscosity η (23 °C) [Pa·s]	2,6	3,1	3,3	4,1
compressive strength [MPa]	238 ± 12	240 ± 11	235 ± 22	225 ± 14
flexural strength [MPa]	60 ± 4	62 ± 4	72 ± 6	69 ± 4
Young's modulus [MPa]	1620 ± 50	1850 ± 50	2180 ± 80	2010 ± 120
yield stress [MPa]	96 ± 2	110 ± 2	115 ± 3	114 ± 1

After removing volatile components, condensation products **CP_{2b}-TEOS-x** were mixed with Bis-GMA/TGDMA and polymerized by means of radicals in order to incorporate the particles in the matrix. Bis-GMA provides the necessary hardness to mill the resulting composites. The characterization of the obtained nanocomposite powders by means of solid state ²⁹Si cross-polarization magic angle spinning (CP MAS) NMR spectroscopy led to the spectrum illustrated in Figure 4, evidencing the high alkoxysilane conversion. The strongest signal at -66.1 ppm results from Si connected through O atoms to three other Si (T³). Another two signals were detected in the range of -100 (Q³) and -110 ppm (Q⁴), supporting the cross-linked structure of the nanoparticles.

C. Composites. Nanocomposites were prepared by blending Bis-GMA/TGDMA (70:30 w/w) with the condensation products **CP_{2b}-TEOS-1**–**CP_{2b}-TEOS-4** (CP: Bis-GMA/TGDMA = 70:30) and 0.75 wt % of the initiator system campherchinone/dimethylaminobenzoic acid ethyl ester (1:1 mol/mol). After photopolymerization, the mechanical data were examined (cf. Table 2). The compressive strength of the nanocomposites was in the range of 110–160 MPa and the flexural strength was in the range of 6–12 MPa, respectively. In comparison with the Bis-GMA/TGDMA without filler both the compressive strengths and the flexural strengths were surprisingly low. Most likely, after storage of the samples over a period of 24 in water, the polymerizates of methacrylates tend to hydrolyze in water and the exposure to water plasticized the materials to the degree that the mechanical properties were effectively lowered.

To examine the role of **4** (Scheme 3) with respect to matrix/filler interaction, composites were prepared by

addition 20 wt % glass filler (Potters Ballotini, microspheres 5000CP-00, average diameter 5 μm, containing 7 wt % calcium ions and 2 wt % magnesium ions) and different amounts of monomer **4** (0–5 wt %) to the matrix resin consisting of Bis-GMA/TGDMA (weight ratio 70:30 w/w). The uncured blend exhibits viscosities in the range 3.1–4.1 Pa·s, whereas the viscosities of the resins increased by adding increasing amounts monomer **4**. After photopolymerization the fractured surfaces of the composites (**FC-MS-0**, **FC-MS-1**, **FC-MS-5**, Table 3) were investigated by means of the environmental scanning electron microscopy (ESEM) to obtain information about the morphology of the composites. As expected, the composite **FC-MS-0** exhibits a very smooth surface reflecting the absence of matrix/filler interaction (Figure 6). However, addition of monomer **4** to composites **FC-MS-1** and **FC-MS-5**, respectively, resulted in matrix/filler interaction. Figure 7 shows the ESEM images of particles with polymer bound on the glass surface. Improved surface adhesion is likely to result from the complexation of calcium and magnesium ions of the filler via the phosphonic acid of monomer **4**. Phosphorus-containing monomers with phosphonic acid were used as dentin adhesives because they can form complexes with the calcium ions in the inorganic components of dentin.^{14,15,19–21}

Viscosities and mechanical properties of the prepared composites are summarized in Table 3. Except for compressive strength, the mechanical properties of the composites with monomer **4** such as flexural strength, Young's modulus and the Yield stress are increased. This is in accord with results in the literature, that the yield behavior of glass filled polymers was dependent on the glass/polymer interfacial adhesion.^{22,23} The substantial improvement of interfacial adhesion is ac-

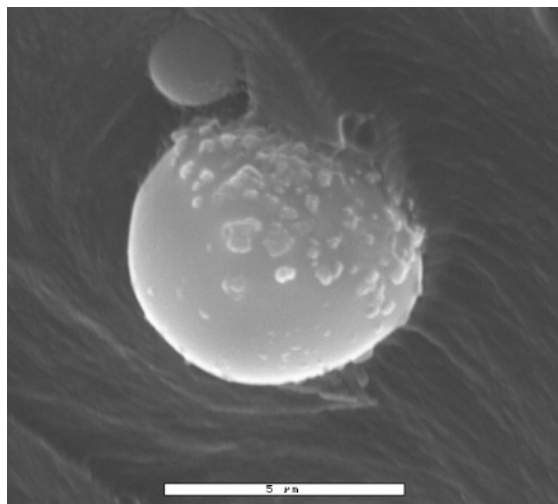
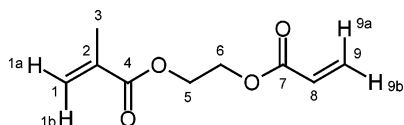


Figure 7. Fracture surface of the composite FC-MS-5.

Scheme 4. Ethylene Glycol Acrylate Methacrylate (EGAMA)



accompanied by only small improvements of 10–15% of flexural strength and 9–18% of Young's modulus. Surprisingly, the best mechanical properties are observed with 1 wt % of monomer **4**. A possible explanation is the lower network formation in the composite FC-MS-5 and the low solubility of ionic monomer **4** in the matrix at 5 wt %. Residual monomer which was not bound to the surface of the fillers can plasticize the composite matrix.^{24, 25}

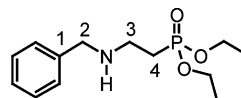
D. Conclusions. Novel phosphonate-functional monomers and silanes containing a methacrylic group were synthesized via single Michael addition of alkylamines to diethyl vinylphosphonate and subsequent condensation with (meth)acryloyl chloride and another Michael addition to 2-(acryloyloxy)ethyl methacrylate, respectively. Thereby, phosphonate-functional silanes are interesting sol-gel precursors for the preparation of hybrid materials like organic/inorganic hybrid nanoparticles. Furthermore, the hydrolysis of the phosphonate group results in a phosphonic acid functional monomer which can be used as component of dental composites exhibiting improved filler-matrix interaction.

Experimental Section

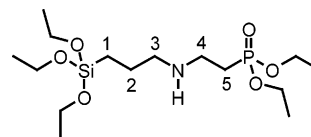
(Aminopropyl)triethoxysilane, benzylamine, diethyl vinylphosphonate (DEVPh), trimethylsilyl bromide, 2-hydroxyethyl methacrylate (HEMA), acryloyl chloride, methacryloyl chloride, campher quinone, ethyl-4-(dimethylamino)benzoate (DMABE), and di-*tert*-butyl-*p*-cresole (BHT) were supplied by Fluka, 2,2-bis-[*p*-(2-hydroxy-3-methacryloyloxypropoxy)phenyl]propane (Bis-GMA), triethylenglycoldimethacrylate (TGDMA) by Röhm, triethylamine by Aldrich, Spheriglas 5000CP-00 (spherical diameter 5 μm) by Potters-Ballotini, and Jeffamine ED 2003 (PEO II) $M_n \approx 1900$ by Huntsman.

Synthesis of 2-(acryloyloxy)ethyl methacrylate (Scheme 4). In a three-necked flask equipped with stirrer, thermometer and dropping funnel 89.88 g (0.691 mol) HEMA and 76.88 g (0.760 mol) triethylamine were dissolved in 500 mL of absolute toluene. Under cooling (0–5 °C) 68.75 g (0.760 mol), acryloyl chloride dissolved in 50 mL of toluene was added

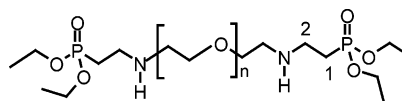
Scheme 5. Amine PA-BA (1a)



Scheme 6. Amine PA-APTES (1b)



Scheme 7. Amine PA-JA (1c)



during 4 h. After the reaction was stirred overnight, the precipitate was filtered off and washed twice with 25 mL of toluene. Then the reaction mixture was extracted twice with 150 mL of water, 100 mL of 1 N HCl, and 100 mL of 1 N Na₂HCO₃ and dried over Na₂SO₄. Thereafter the toluene was distilled off (32 mbar 40 °C) and 100 mg of BHT were added.

IR: 1726 cm⁻¹ (s, C=O), 1638 cm⁻¹ (m, C=C).

¹H NMR: δ = 6.42 (9a, d), 6.11 (1b, 8, m), 5.83 (9b, d), 5.57 (1a, s), 4.39 (5, 6, s), 1.93 (3, s).

¹³C NMR: δ = 167.1 (4), 165.9 (7), 135.9 (2), 131.4 (9), 128.0 (8), 126.1 (1), 62.4 (6), 62.2(5), 18.3 (3).

General Procedure for the Preparation of Secondary Amines PA-X. To a solution of diethyl vinylphosphonate (11 mmol) in 5 mL of absolute ethanol, the appropriate amine (10 mmol) dissolved in 5 mL of absolute ethanol was added. After the mixture was stirred for 24 h at 70 °C, colorless oils (**1a** and **1b**) or a solid (**1c**) were obtained by distillation of the solvent and characterized by mass spectrometry, GC, ¹H NMR, and ¹³C NMR.

Amine PA-BA (1a) (Scheme 5). C₁₃H₂₂NO₃P (271.30): *m/z* (GC-MS) = 372 [MH⁺]. RT (GC): 27.5 min.

¹H NMR: δ = 7.21–7.29 (m, aromatic H), 3.99–4.11 (m, POCH₂CH₃), 3.77 (s, 2), 2.90 (td, 3), 1.92–2.03 (m, 4), 1.27 (t, POCH₂CH₃).

¹³C NMR: δ = 140.0 (1), 128.4 (aromatic C), 62.1 (POCH₂-CH₃), 52.9 (2), 43.7 (3), 27.1 (d, 4), 17.0 (POCH₂CH₃). ³¹P NMR: δ = 31.8 (s).

Amine PA-APTES (1b) (Scheme 6). C₁₅H₃₆NO₆PSi (385.52): *m/z* (GC-MS) = 386 [MH⁺]. RT (GC): 28.8 min;

¹H NMR: δ = 3.98–4.05 (m, POCH₂CH₃), 3.78 (q, SiOCH₂-CH₃), 2.81 (td, 4), 2.52 (t, 3), 1.85–1.94 (m, 5), 1.40–1.61 (m, 2), 1.23 (t, SiOCH₂CH₃), 1.13 (t, POCH₂CH₃), 0.54 (t, 1).

¹³C NMR: δ = 62.1 (POCH₂CH₃), 58.8 (SiOCH₂CH₃), 52.9 (3), 43.7 (4), 27.1 (d, 5), 23.8 (2), 18.9 (SiOCH₂CH₃), 17.0 (POCH₂CH₃), 8.5 (1). ³¹P NMR: δ = 30.5 (s).

Amine PA-JA (1c) (Scheme 7). ¹H NMR: δ = 3.96–4.03 (m, POCH₂CH₃), 3.56 (s, OCH₂CH₂O, OCH₂CH₂N), 2.69–2.91 (m, 2), 1.88 (td, 1), 1.24 (t, POCH₂CH₃).

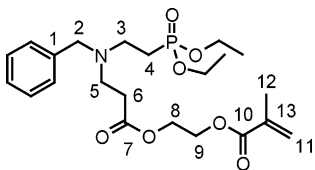
¹³C NMR: δ = 70.4 (OCH₂), 62.1 (POCH₂CH₃), 52.3 (NCH₂), 40.5 (2), 26.8 (d, 1), 17.1 (POCH₂CH₃). ³¹P NMR: δ = 29.4 (s).

General Procedure for the Preparation of the Hybrid Monomers MA-PA-BA and MA-PA-APTES. Ethylene glycol acrylate methacrylate (EGAMA) (10 mmol) was added slowly to a solution of the appropriate amine (10 mmol) in 10 mL of absolute ethanol. The mixture was stirred at 25 °C for 2 h. Then the ethanol was distilled off and the mixture was stirred for a further 48 h at 23 °C.

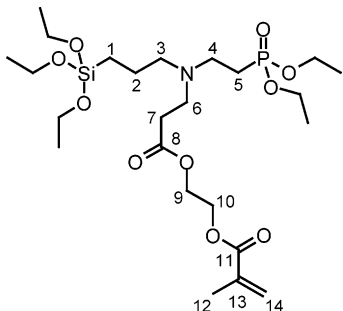
Hybrid Monomer MA-PA-BA (2a) (Scheme 8). C₂₂H₃₄NO₇P (455.49), *m/z* (FAB-MS) = 456 [MH⁺].

¹H NMR: δ = 7.17–7.24 (m, aromatic H), 6.09, 5.48 (d, 11), 4.21 (s, 8, 9), 3.90–3.99 (POCH₂CH₃), 3.73 (s, 2), 2.84 (td, 3), 2.71 (t, 5), 2.40 (t, 6), 1.90–2.10 (m, 4), 1.82 (s, 12), 1.16 (t, POCH₂CH₃).

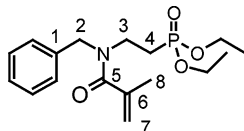
Scheme 8. Hybrid Monomer MA-PA-BA (2a)



Scheme 9. Hybrid Monomer MA-PA-APTES (2b)



Scheme 10. Hybrid Monomer MAA-PA-BA (3a)



^{13}C NMR: $\delta = 171.8$ (7), 166.6 (10), 140.0 (1), 135.5 (13), 128.4 (aromatic C), 125.6 (11), 62.2 (POCH_2CH_3), 61.9 (9), 61.7 (8), 52.9 (2), 48.4 (5), 43.7 (3), 32.2 (6) 27.1 (d, 4), 18.0 (12), 17.0 (POCH_2CH_3).

^{31}P NMR: $\delta = 31.1$ (s).

Hybrid Monomer MA-PA-APTES (2b) (Scheme 9). $\text{C}_{24}\text{H}_{48}\text{NO}_{10}\text{PSi}$ (569.71), m/z (FAB-MS) = 570 [MH^+].

^1H NMR: $\delta = 6.03$, 5.45 (d, 14), 4.17 (s, 9, 10), 3.84–4.00 (m, POCH_2CH_3), 3.64 (q, $\text{SiOCH}_2\text{CH}_3$), 2.55–2.68 (m, 4, 6), 2.20–2.36 (m, 3, 7), 1.77 (s, 12), 1.66–1.82 (m, 5), 1.29–1.42 (m, 2), 1.15 (t, $\text{SiOCH}_2\text{CH}_3$), 1.04 (t, POCH_2CH_3), 0.40 (t, 1).

^{13}C NMR: $\delta = 171.8$ (8), 166.6 (11), 135.5 (13), 125.6 (14), 62.1 (POCH_2CH_3), 61.9 (10), 61.7 (9), 57.9 ($\text{SiOCH}_2\text{CH}_3$), 55.7 (3), 52.9 (2), 48.4 (6), 43.7 (3), 32.2 (7) 27.1 (4), 22.8 (d, 5), 20.0 (2), 18.0 (12), 17.9 ($\text{SiOCH}_2\text{CH}_3$), 16.6 (POCH_2CH_3), 7.4 (1); ^{31}P NMR: $\delta = 32.8$ (s). ^{29}Si NMR: $\delta = -44.6$.

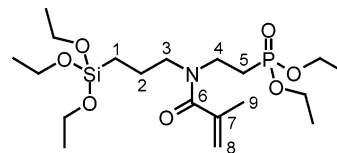
Hybrid Monomer MAA-PA-BA (3a) (Scheme 10). In a three-necked flask equipped with stirrer, thermometer, and dropping funnel PA-BA (3.732 g, 0.014 mol), triethylamine (1.531 g, 0.015 mol) and DMAP (0.126 g, 0.001 mol) were dissolved in 20 mL of dry dichloromethane. Under cooling (0–5 °C), methacryloyl chloride (1.582 g, 0.015 mol) dissolved in 10 mL of dry dichloromethane, was added during 1 h. After the mixture was stirred overnight, the obtained precipitate was filtered off and washed twice with 20 mL of dichloromethane. Then the reaction mixture was extracted with 50 mL of water, 50 mL of 1 N HCl, and 50 mL of 1 N NaHCO_3 and dried over Na_2SO_4 . Subsequently, dichloromethane was evaporated.

$\text{C}_{22}\text{H}_{34}\text{NO}_7\text{P}$ (340.21). ^1H NMR: $\delta = 7.17$ –7.50 (m, aromatic H), 5.20 (d, 7), 4.70 (s, 2), 4.05–4.20 (m, POCH_2CH_3), 3.65 (td, 3), 1.95–2.20 (m, 4, 8), 1.30 (t, POCH_2CH_3).

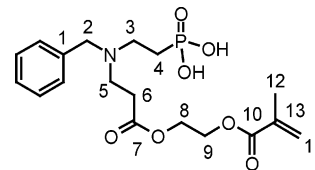
^{13}C NMR: $\delta = 171.7$ (5), 139.4 (1), 140.0 (1), 135.6 (6), 125.9–127.7 (aromatic C), 114.5 (7), 60.6 (POCH_2CH_3), 52.4 (3), 38.5 (2), 22.6 (d, 4), 19.5 (8), 15.3 (POCH_2CH_3); ^{31}P NMR: $\delta = 29.5$ (s).

Hybrid Monomer MAA-PA-APTES (3b) (Scheme 11). The appropriate amine PA-APTES (8.924 g, 0.023 mol), triethylamine (2.577 g, 0.025 mol) and DMAP (0.212 g, 0.002 mol) were dissolved under Ar in 60 mL of dry dichloromethane. Under cooling (0–5 °C), methacryloyl chloride (1.582 g, 0.015 mol) dissolved in 20 mL of dichloromethane was added during 1 h. After the mixture was stirred overnight, the precipitate was filtered off. Dichloromethane was evaporated and column

Scheme 11. Hybrid Monomer MAA-PA-APTES (3b)



Scheme 12. Hybrid Monomer MA-Phosphonic Acid-BA (4)



chromatography of the residue on Al_2O_3 ($\text{MeOH}:\text{CHCl}_3 = 1:1$) yielded the desired amide.

$\text{C}_{24}\text{H}_{48}\text{NO}_{10}\text{PSi}$ (454.09). ^1H NMR: $\delta = 5.03$ (d, 8), 4.05–4.09 (m, POCH_2CH_3), 3.76 (q, $\text{SiOCH}_2\text{CH}_3$), 3.45–3.60 (m, 4), 3.28 (t, 3), 1.95–2.15 (m, 5), 1.90 (s, 9), 1.50–1.70 (m, 2), 1.31 (t, $\text{SiOCH}_2\text{CH}_3$), 1.17 (t, POCH_2CH_3), 0.48 (t, 1).

^{13}C NMR: $\delta = 172.7$ (6), 140.9 (7), 114.8 (8), 61.9 (POCH_2CH_3), 58.5 ($\text{SiOCH}_2\text{CH}_3$), 51.8 (3), 39.7 (4), 24.1 (d, 5), 22.7 (6), 20.6 (9), 18.3 ($\text{SiOCH}_2\text{CH}_3$), 16.5 (POCH_2CH_3), 7.6 (1). ^{31}P NMR: $\delta = 31.8$ (s).

Hybrid Monomer MA-Phosphonic Acid-BA (4) (Scheme 12). Trimethylsilyl bromide (3.062 g, 20 mmol) was added slowly to a solution of **3** (4.104 g, 9 mmol) in 20 mL of absolute dichloromethane. After being stirred under reflux for 1.5 h, excess trimethylsilyl bromide and the solvent were removed by rotary evaporation. The residue was then dissolved in 20 mL of methanol, and a white crystalline product precipitated after stirring for 48 h.

$\text{C}_{18}\text{H}_{26}\text{NO}_7\text{P}$ (399.38). ^1H NMR (D_2O): $\delta = 7.17$ –7.24 (m, aromatic H), 5.88, 5.40 (d, 11), 4.21 (s, 8, 9), 3.73 (s, 2), 2.84 (3), 2.71 (t, 5), 2.40 (t, 6), 1.90–2.10 (m, 4), 1.74 (s, 12).

^{13}C NMR (D_2O): $\delta = 171.8$ (7), 166.6 (10), 140.0 (1), 135.5 (13), 128.4 (aromatic C), 125.6 (11), 61.9 (9), 61.7 (8), 52.9 (2), 48.4 (5), 43.7 (3), 32.2 (6) 27.1 (d, 4), 18.0 (12).

^{31}P NMR (D_2O): $\delta = 19.2$ (s).

Sol-Gel Condensation of MA-PA-APTES (2b) in ethyl acetate (CP_{2b}). **2b** (2.00 g, 3.5 mmol) and ethyl acetate (7.80 g) were mixed. Initiation of the sol-gel condensation was achieved by adding this mixture to a solution of aqueous HF (3%) (0.195 g, 10.5 mmol H_2O). After the mixture was stirred for 2 days at ambient temperature, volatile components were removed under vacuum for 1 h.

Sol-Gel Condensation of MA-PA-APTES (2b) with TEOS (CP_{2b-TEOS-x}). The hybrid monomer MA-PA-APTES (5.50 g, 0.010 mol) and TEOS (0.5 g, 0.002 mol) were mixed with a solution of aqueous HF (3%) (0.716 g, 0.039 mol H_2O) in ethyl acetate (3.284 g, 0.037 mol) to start the condensation reaction of alkoxy silane groups. Three moles of water per mole of alkoxy silane provided rapid condensation reactions. The reaction mixture was stirred at room temperature for 2 days to obtain full condensation.

Preparation of the Composites. Polymerizable matrix resins were prepared by mixing Bis-GMA/TGDMMA (70:30) with the condensation products $\text{CP}_{2b-\text{TEOS}-x}$ ($\text{CP}_{2b-\text{TEOS}-x}$: Bis-GMA/TGDMMA = 70:30) and 0.75 wt % of the initiator system campherchinone/dimethylaminobenzoic acid ethyl ester. Further polymerizable matrix resins were prepared by mixing Bis-GMA/TGDMMA (70:30) with microspheres (average particle size: 5 μm , Potters Ballotini, 5000CP-00) and **4** (molar ratio: Table 1). In this case campherchinone/dimethylaminobenzoic acid ethyl ester (0.75 wt %) was also used as initiator system. All mixtures were degassed at 200 mbar and 60 °C for 30 min and homogenized by stirring at room temperature for 1 h.

Preparation of the Test Specimens. Cylindrical test specimens were made by placing the mixed polymerizable matrix resins into stainless steel molds (height 6 mm, diameter

4 mm), then slightly overfilling them and gently compressing them between two glass plates. The specimens were polymerized with a curing device (Spektrum 800, wavelength (λ_{\max}) = 465 nm, light intensity 800 mW/cm²) for 40 s on both ends of the specimens. Rod like test specimens (height and width 2 mm, length 2.5 mm) were prepared in the same manner except for the polymerization procedure. Photochemical polymerization was carried out in a Triad photochemical curing unit (λ_{\max} = 470 nm, Dentsply De Trey, Konstanz, Germany) within 3 min on both ends of the specimens. All test specimens were gently removed from the molds and stored in deionized water at 37 °C for 24 h before testing.

Methods. NMR. ¹H, ¹³C and ³¹P NMR spectra were recorded in CDCl₃ at concentrations of 250 g/L on a Bruker ARX 300 spectrometer, operating at 300, 75.4, and 59.6 MHz, respectively.

The solid state ²⁹Si CP MAS NMR spectra was run on a Bruker Avance 500 spectrometer at 99.3 MHz with cross-polarization on samples spun at 10 kHz.

Viscosities. Rheological properties were determined using a Bohlin CS50 rheometer with water-bath temperature control. Cone-and-plate geometry was used with 1.5 cm³ being transferred to the plate at room temperature. Measurements viscosity were made with the instrument in continuous-shear mode, with at least 10 min allowed at room temperature for equilibration.

FAB-MS. Fast atom bombardment mass spectra were obtained with a double focusing Finnigan MAT 312/AMD 5000 mass spectrometer equipped with a Cs ion source.

GC-MS. Measurements were carried out with a Thermo Quest Trace 2000 Series GC connected with Voyager GC/MS of Thermo Quest Finnigan. Spectra were recorded in MeOH at concentrations of 5 wt %.

MALDI-TOF. (matrix assisted laser desorption ionization-time of light) spectra were obtained with a REFLEX II mass spectrometer (Bruker-Franzen). Appropriate amounts of matrix (cyanohydroxy cinnamic acid) and polymer was dissolved in CHCl₃. The metal ion Li⁺ often required for enhanced cationization was added as their inorganic salt (LiCl), and 1 μ L of the whole solution was then applied to a sample holder and allowed to dry. The resulting homogeneous solid mixture was then introduced into the ion source of the mass spectrometer and irradiated by a pulsed UV laser (accelerating voltage 20 kV).

Mechanical Data. The compressive strengths and yield stresses were tested using the method "compression test with yielding point" according to the ISO 9917 and determined with a Zwick testing machine Z010. The specimens were placed with their flat ends between the plates of the testing machine, so that compressive load was applied along the long axis of the specimens. The force-displacement curve was analyzed with testXpert (version 10.11) software to obtain the yield stress. The compressive strength was calculated from the maximum applied load. The flexural test was performed according to ISO 4049 using a Zwick instrument Z010. The flexural strengths was calculated from the maximum load. Analyzing the force-displacement curve with testXpert software resulted in Young's modulus.

Transmission Electron Microscopy (TEM). The samples were prepared by dropping solutions of nanoparticles on carbon grids. After drying in a vacuum homogeneous films were obtained. The TEM measurements were carried out with a LEO CEM 912 transmission electron microscope applying an acceleration voltage of 120 kV.^{26,27} The particle size was determined by the analysis of numerous TEM images using the iTEM-software of SIS.

Environmental Scanning Electron Microscope (ESEM). The ESEM measurements of fractured surfaces of the composites were carried out with a ESEM 2020 environmental scanning electron microscope applying a LaB₆-cathode and an acceleration voltage of 23 kV. The images were obtained by gaseous secondary electron detector at pressures of 666–1067 Pa.²⁸

References and Notes

- (1) Cook, W. D.; Tyas, M. J. *Biomaterials* **1985**, *6*, 362.
- (2) Bowen, R. L.; Marjenhoff, W. A. *Adv. Dent. Res.* **1992**, *6*, 44.
- (3) Bowen, R. L.; Marjenhoff, W. A. US Patent 3,066,112.
- (4) Nunes, T. G.; Pires, R.; Perdigao, J.; Amorim, A.; Polido, M. *Polymer* **2001**, *42*, 8051.
- (5) Schmidt, H. *CHIUZ* **2001**, *35*, 176.
- (6) Paul, P. P. US Patent 6,005,028.
- (7) Müh, E.; Frey, H.; Klee, J. E.; Mülhaupt, R. *Adv. Funct. Mater.* **2001**, *11*, 425.
- (8) Müh, E.; Marquardt, J.; Klee, J. E.; Frey, H.; Mülhaupt, R. *Macromolecules* **2001**, *34*, 5778.
- (9) Müh, E.; Weickmann, H.; Klee, J. E.; Frey, H.; Mülhaupt, R. *Macromol. Chem. Phys.* **2001**, *202*, 3484.
- (10) Müh, E.; Stieger, M.; Klee, J. E.; Frey, H.; Mülhaupt, R. *J. Polym. Sci.: Part A: Polym. Chem.* **2001**, *39*, 4274.
- (11) Mou, L.; Singh, G. J.; Nicholson, W. *Chem. Commun.* **2000**, 345.
- (12) Zeuner, F.; Moszner, N.; Völkel, T.; Vogel, K.; Rheinberger, V. *Phosphorus, Sulfur Silicon* **1999**, *144–146*, 133.
- (13) Moszner, N.; Zeuner, F.; Rheinberger, V. *Macromol. Symp.* **2001**, *175*, 133.
- (14) Moszner, N.; Zeuner, F.; Fischer, U.; Rheinberger, V. *Macromol. Chem. Phys.* **1999**, *200*, 1062.
- (15) Moszner, N.; Zeuner, F.; Pfeiffer, S.; Schurte, I.; Rheinberger, V.; Drache, M. *Macromol. Mater. Eng.* **2001**, *286*, 225.
- (16) Moszner et al., N. *Macromol. Chem. Phys.* **1996**, *197*, 81.
- (17) Rodriguez et al., S. *Tetrahedron* **2002**, *58* (6), 1185.
- (18) Moszner, N.; Völkel, T.; Cramer von Clausbruch, S.; Geiter, E.; Batliner, N.; Rheinberger, V. *Macromol. Mater. Eng.* **2002**, *287*, 339.
- (19) Nakabayashi, N.; Kanda, K. *J. Dent. Mat.* **1987**, *6*, 396.
- (20) Nikaido, T.; Nakabayashi, N. *J. Dent. Mat.* **1987**, *6*, 690.
- (21) Fusayama et al., T. *J. Dent. Res.* **1979**, *58*, 1364.
- (22) Dekkers, M. E.; Heikens, D. *J. Mater. Sci.* **1984**, *19*, 3271.
- (23) Kawaguchi, T.; Raymond, R. A. *Polymer* **2003**, *44*, 4229.
- (24) Pukanszky, B.; Tüdös, F. *Macromol. Chem., Macromol. Symp.* **1989**, *28*, 16.
- (25) Pekete, E.; Pukanszky, B.; Toth, A. *J. Colloid Interface Sci.* **1990**, *135*, 200.
- (26) Sawyer, L.; Grubb, D. *Polymer Microscopy*, Chapman and Hal: new York, 1987.
- (27) Gruehn, R.; Ross, R. *CHIUZ* **1987**, *18*, 813.
- (28) Cameron, R. *TRIP* **1994**, *2*, 116.

MA047526E